Physicochemical and Structural Effects of Electrolyte-Induced Delamination on Polyethylene Teraphthalate-Coated Steel Plates

E. Zumelzu,[1] C. Ortega,[2] F. Rull,[3] C. Cabezas[4]

[1]*Instituto de Materiales y Procesos Termomecánicos, Universidad Austral de Chile, Casilla 567, Valdivia, Chile*
[2]*Escuela de Mecánica, Facultad de Ciencias de la Ingeniería, Universidad Austral de Chile, Valdivia, Chile*
[3]*Dpto. Física de la Materia Condensada, Cristalografía y Mineralogía, Universidad de Valladolid, Spain*
[4]*Instituto de Química, Universidad Austral de Chile, Valdivia, Chile*

Received 26 October 2009; accepted 29 March 2011
DOI 10.1002/app.34588
Published online 19 August 2011 in Wiley Online Library (wileyonlinelibrary.com).

ABSTRACT: This research evaluated the *in situ* physicochemical changes and alterations occurring in an electrolytic chromium coated steel (ECCS), surface protected by polyethylene teraphthalate (PET) copolymer, after inducing a fracture on the coating in an acid acetic-acetate medium. The delamination was characterized in the front of the failure by means of anodic and cathodic electrochemical mechanisms, and the resistance and degradation of the metal-polymer composite's substrates were analyzed by means of Raman vibrational spectroscopy. The application of an electrochemical cell to generate *in situ* delamination, simulating the formation of pores or artificial defects, provided information on the activity inside the substrates of the PET-coated ECCS composite as a result of the effect of the acetic acid. The anodic delamination mechanism is based on the diffusion of the electrolyte through the metal-polymer interface and the pre-existence of pores on the polymer layer. The cathodic delamination mechanism is based on the mechanical action of the gaseous hydrogen as a result of the reduction of H^+. © 2011 Wiley Periodicals, Inc. J Appl Polym Sci 123: 1658–1666, 2012

Key words: degradation; PET; ECCS; induced detachment; Raman spectroscopy; adhesion

INTRODUCTION

Polymer-coated plates have shown a great development, resulting in new knowledge-intensive products for use in applications at the automobile industry and food containers.[1–5] The latter sector faces more and more the pressures and regulations of food safety and industrial ecoefficiency, with rigorous certification regulations and directions of great impact on the canning industry to ensure the quality of their products.[6]

The metal-polymers plates are intended to replace the conventional steel containers coated with sanitary lacquers, due to the minimum emission of solvents and chemical elements when compared with the traditional lacquers.

In this sense, the electrolytic-chromium coated steels (ECCS), surface-protected by a polyethylene teraphthalate (PET) corolled layer, are multifunctional advanced materials that incorporate an improved protection-barrier effect and are more environmental-friendly in their manufacturing processes.

There are several reasons for the weak cohesion of interfacial layers: contamination caused by air bubbles, dust, and humidity, which have not been eliminated from the surface of the substrate and low-molecular weight substances or additives that migrate to the interface once the joint has formed. According to the above-mentioned, generally speaking the adhesion depends on the chemical surface and physical nature of the polymer coating and metal substrate, as well as on the interactions between them at the interface level.[7,8]

Regarding PET-coated ECCS plates, the adhesion is mainly explained by its structural constituents. It is well known that the chromium deposit on the ECCS plate consists of Cr° and $Cr^\circ + Cr^{n+}$ ($n = 2$, 3). Polyethylene teraphthalate is manufactured by the polycondensation reaction of ethylene glycol and dimethyl teraphthalate. To achieve the metal-polymer bonding, the chromium uses the oxygen of the PET to form links similar to those of the oxide with which good adhesion of the polymer to the ECCS plate can be achieved.

A bonding model that would explain the adhesion of the metal-polymer laminate is that of the acid-base interaction mechanism. In this model on the

Correspondence to: E. Zumelzu (ezumelzu@uach.cl).
Contract grant sponsor: Fondecyt Project; contract grant number: 1070375.

PET-coated ECCS plate, the carbonyl oxygen shares (electron pair donor = base) its electrons with chromium (electron pair acceptor = acid). A similar argument can be used with the electrons of the benzene ring and chromium.

In the chromium-benzene ring chemical bonding, there are four chromium electrons (Cr^{2+}), i.e., two electrons from each oxygen atom in both carbonyls. The benzene ring of the PET contributes up to six electrons in pairs according to the structure of the delocalized orbitals of benzene. As the oxygen molecules come closer, the Cr^{2+} acts like an acid and the benzene ring and oxygen atoms like a base, and the electrons exchange giving rise to covalent bonds. This explains the strong adherence between the PET coating and the chromium deposit on the ECCS plate.

The delamination of polymer protective coatings on metals, under humid environments, is associated to a complex number of physicochemical phenomena.[9–14] One of the widely accepted mechanisms is that the reaction forces involve the formation of electrochemical microcells with different anodic and cathodic zones which lead to detachment. These can cause metallic corrosion products at the metal-polymer interface level, which due to volume changes exert surface pressures facilitating delamination. The former is facilitated by various factors like sanitary processes such as pasteurization, aggressiveness of the electrolytes, and thickness of the coating, among others.

On the other hand, it is important to achieve cohesive chemical and mechanical bonds at the metal-polymer interface to prevent detachments. In this sense, the thermal treatments applied during the manufacturing of PET-ECCS colaminates generate amorphous cross-sectional PET structures at the interface level,[15] favoring anchoring to the chromium oxide substrate of steel due to the disarrangement of the PET polymer chains. Such morphology induces a suitable interaction between the polymer chains and chromium substrate on the steel plate through an amorphous morphology at the metal-polymer interface level. Due to manufacturing defects, small areas of the steel surface remain unprotected by the Cr_2O_3 layer, and the presence of pores in the PET polymer both allow the direct contact between the steel and PET coating, favoring the acid-steel interaction, and generating steel corrosion.[15,16]

Particularly, it has been found that the acetic acid degrades the polyethylene teraphthalate (PET) coatings, protecting the electrolytic-chromium coated steels (ECCS), under certain conditions of concentration, temperature, and time. An important factor to prevent degradation is to provide an adequate continuity and permeability of the PET layer by ensuring it is free from pores, loops, deformations, marks, scratches, and other defects resulting from the corolling and mechanical forming processes of containers.[17–20]

This work addresses experimental studies on the induced delamination of the PET polymer protecting the ECCS plate, especially in the initial stages of the delamination process; in this connection, an artificial surface defect or surface crack on the PET coating in an acetic-acetate electrolytic medium is produced to study the anodic and cathodic behaviors.

This simulation is intended to show the physicochemical mechanisms involved in the delamination of the composite and to determine the degradation of the protective PET coating. On the other hand, an evaluation of the effect of the acetic-acetate medium on the polymer and on the distribution of TiO_2 pigments that provide the PET color is also attempted, as well as a determination of changes in the chemical composition or in the structural arrange of the coating by means of vibrational spectroscopy. Likewise, a characterization of the "*in situ* evolution" of the composite's substrate degradation, at an optical and microstructural level, is also an objective, to determine the critical factors that lead to the detachment onset, spreading, and damages involved in the material layers resulting from the electrolyte attack.

In this regard, the literature evaluates the aging of containers (metal/lacquer), in relation with the delamination processes, by means of the use of electrochemical tests, but provides little information on the degradation of films.[11,16]

MATERIALS AND METHODS

Complex and multifunctional metal-polymer materials were investigated, considering physicochemical aspects in association with performance qualities,[21] to know their resistance and lifespan in aggressive media representative of food containers

The material under study was a PET corolled ECCS composite layer formed by an average 0.20 mm thick ECCS temper base steel coated by a layer generated by electrolytic deposition and consisting of a 0.01 μm thick chromium Cr° and chromium oxide Cr_2O_3 with an average thickness of 0.01 μm, and a total chromium content of 101.33 mg/m^2. The chemical composition (% wt) of steel was: 0.074% C, 0.260% Mn, 0.021% P, 0.016% S, 0.012% Si, 0.032% Al, 45 ppm N, and Fe (remaining percent).

This ECCS steel plate had a 30-μm thick layer of polyethylene teraphthalate (dimethyl teraphthalate + ethylene glycol) to protect the steel against the aggressive nature of the acetic-acetate medium and to ensure continuity in the presence of pores, and whose thickness had no influence on adhesion due to its viscoelastic behavior; an amorphous structure at the metal interface level to favor adhesion; a biaxial orientation in the rest of its thickness to ensure

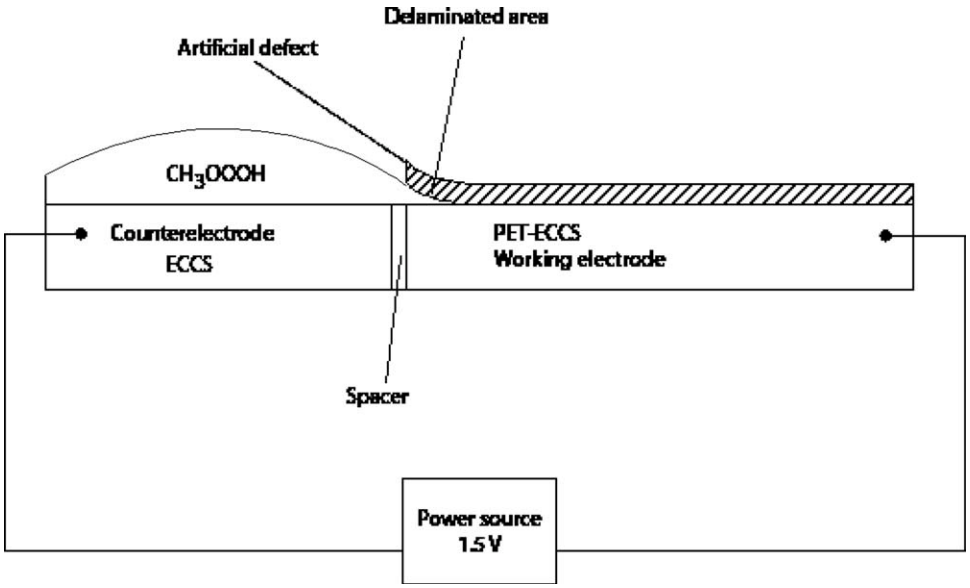

Figure 1 Simplified scheme of delamination trial.

good abrasion and degradation resistance properties in a medium representative of canned foods; and TiO_2 pigments that provided the white color to improve the sanitary appearance.

As depicted in Figure 1, the induced-delamination experiments employed two 15 mm wide and 210 mm long coupons facing each other by the cross section area, and were separated only by a 0.45 mm industrial plastic spacer. One of the coupons was a flat, PET corolled ECCS plate and had an existing artificially-made surface defect 15 × 140 mm in size, and acted as the working electrode. The former simulated the discontinuity found in a polymer coating, and was deep enough to reach the metal substrate and expose the interface to the electrolyte, making it susceptible to delamination. The other coupon consisted of a flat, non-PET coated ECCS plate, and acted as the counterelectrode.

Both plates and the spacer were placed in a hollowed industrial plastic matrix, which allowed for the addition of electrolyte, consisting of 0.1 g/L acetic acetate buffer solution at pH 3.85, and limited its contact to the surface of the counterelectrode and to the cross section area of the working electrode, preventing the electrolyte to flow on the sides.

After mounting of the plates on the sample holder, they were carefully washed with deionized water and then dried out. Later, a thin 10 mL layer of electrolyte (acetic acetate) was deposited on the surface of the counterelectrode up to the spacer and cross section area of the working electrode to allow contact between the electrolyte and the PET-ECCS working electrode, which was the area of interest, while the rest of the surface of the polymer-coated plate remained dry. The ends of both electrodes were connected to a power source to provide a constant potential of ±1.5V to force the non-PET coated ECCS plates acting as counterelectrodes, to react anodically or cathodically depending on the imposed polarity.

This experiment was to move the electrolyte forward to the front area of the working electrode from the counterelectrode, forcing detachment of the PET at the polymer-steel interface. Both the anodic and cathodic experiments were performed under the same time and voltage conditions. The anode was represented in both experiments by the PET-coated ECCS plate, and the non-PET coated steel plate represented an artificial surface defect, i.e., the bottom of a pore induced by the PET coating fracture.

The polarization experiments lasted 24 h with observations at different time intervals (1, 6, 18, and 24 h). Both experiments were illuminated by cold light, and monitored all the time by a Leica DFC 290 camera assembled on a Leica S6D magnifying glass with an optical zoom of 6.3× to 40×. The former device was employed to take *in situ* photographs every 30 min in the first experiment and every 1 min in the second, and to keep record of the electrochemical attack from the beginning to the end of the experiments, such as the border advance of the electrolyte under the polymer and the possible visible damages.

The chemical composition and structural evaluations of the metal-polymer composite, after the induced-delamination experiment, were carried out by means of vibrational spectroscopy (Raman and micro-Raman) analyses.

Vibrational spectroscopy is a methodology that studies the interaction between electromagnetic radiation and material samples. It is based on the

spectral analysis to detect the absorption or emission of electromagnetic radiation at certain wavelengths, and to relate these with the levels of energy involved in a quantum transition.

When the effect of light dispersion occurs, most of the energy particles (photons) are scattered without changes, neither in their energy content nor in their frequency. This is known as the Raleigh scattering effect or elastic scattering. A small fraction of the light dispersed (approximately between 1 and 10 photons for every million) suffers a change in the wave number (reciprocal value of wavelength) in which it vibrates. This change is known as the Raman effect or inelastic Raman scattering, and is the principle on which the Raman spectroscopy is based. These changes correspond to alterations in the vibrational or rotational states of the molecules of the material and are highly specific for each type of molecule. This allows the construction of a (x, y) plot (Raman spectrum) which represents the intensity distribution of the scattered energy for each wave number (Raman shift) within the range evaluated. Each peak of this distribution can be assigned to a particular vibration of the chemical bonds of the material analyzed.

The Raman instrument used in this study consists of a spectrometer (Kaiser Holospec f/1.8i, spectrum range 100–3800 cm^{-1}, and a spectral resolution of 4 cm^{-1}); a CCD detection system (Andor DV420A-OE-130); and an illumination source consisting of a helium-neon (He-Ne) laser at 632′8 nm (Melles-Griot 0.5-lhp-151). This Raman instrument is coupled by optical fiber to a microscope to analyze the samples at a micro scale up to several microns. The samples were examined by making the laser beam strike perpendicular and parallel to the surface. In the perpendicular case, macro mode analyses of the samples using an FT-Raman instrument were performed. Also, cross sections of the samples were microanalyzed parallel to the coating by means of the Raman instrument obtaining spectra every 5 μm at different points starting from the PET surface until reaching the ECCS interface. The diameter of the laser spot was 10 microns approximately. At the polymer-metal interface, spectra were taken focusing the laser spot on the polymer.

Spectral data treatment was performed using both commercial and our own software to correct fluorescence effects and to improve the spectral quality (mainly base line correction, intensity and position calibration, and smoothing). For quantitative spectral analysis the spectra were normalized by area to 1 in the spectral range of interest.[2]

RESULTS AND DISCUSSION

The anodic experiments evidenced three clear stages: stage 1 showed no apparent reaction; stage 2 showed bubbling in the cathode area and small bubbles on the polymer; and stage 3, large bubbling broke loose in the cathode zone, and the reddish color of the anodic area mixed with the buffer.

The degradation observed corresponds to the oxidation of the sample or working electrode, which occurs through the formation of Fe^{2+} ions that give a red coloring to the surrounding electrolytic medium. The delamination of the polymer can be interpreted by the loss of its anchoring to the surface of the solid because of the formation of corrosion spots. These spots allow for the electrolyte or acid to penetrate between the metal and the polymer coating and to appear in the pores of the PET, forming blisters, facilitating its diffusion, and contributing to the delamination of the protective coating.

The 24 h cathodic experiment clearly showed bubbling in the cross section area of the PET-ECCS plate since the beginning (working electrode), typical of the reaction between the electrolyte and the cathode. The electrolyte present in the counterelectrode only had contact with the working electrode in the cross-section area, and since this electrode was induced to react cathodically the bubbles were observed in the front area in addition to the formation of the reddish color typical of the oxide which mixed with the electrolyte. The accelerated anodic attack of the counter-sample without polymer coating caused the reduction of protons in the electrolyte on the metal front of the protected steel plate, and the appearance of hydrogen atoms, which later collaborated in the formation of diatomic molecules that finally were released to form bubbles that mechanically provoked the detachment of the polymer from the metal surface of the working sample, but so would a local pH change due to the depletion of protons and the formation of radicals at the surface. The more the electrolyte penetrates between the polymer coating and the steel the greater the delamination of the coated plate will be.

The cathodic polarization, since the beginning to the end of the experiment, showed the only effect of producing a constant bubbling and release of reddish color into the medium.

Figure 2 shows a comparison of both the anodic and cathodic mechanisms in the acetic-acetate medium for the composite, and indicates the behavior of the PET-ECCS samples after 24 h in the abovementioned conditions.

The cathodic sample showed a hollowed area in the rim, where the maximum length reached was 388.6 μm, measured from the rim and extending over the whole front of the sample; differing from the anodic sample where no apparent depression was observed. This is a defect caused by the bulging or swelling of the protective layer and the acceleration of the hydrogen release resulting from the cathodic experiment.

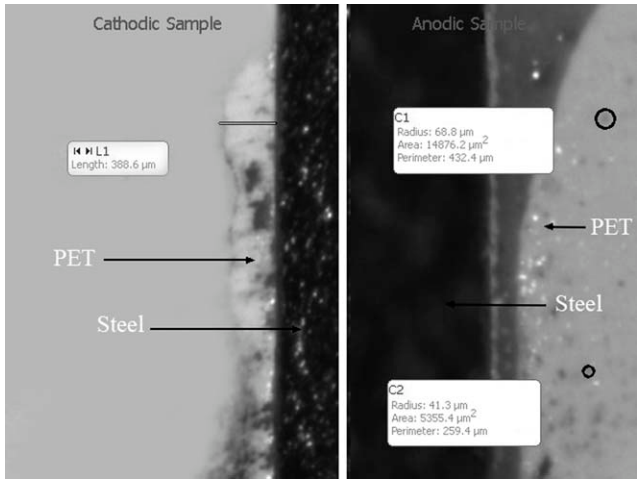

Figure 2 Comparison between anodic and cathodic trials. The cathodic sample exhibits a swollen area extending over the whole surface of the sample; the PET layer is highly degraded. In contrast, the anodic sample shows no apparent bulging; however, there are corrosion spots and oxide formation on the steel, which pushes and separates the protective PET coating from the base steel with changes in morphology and thickness of the PET.

In the anodic sample on the right of Figure 2, the reddish color left by the buffer and the small red spots product of the bubbling, whose radius is that indicated in C1 and C2, can be observed.

Unlike the cathodic sample, there were only red stains or possible outbreaks of pores that reacted during the experiment, in addition of a large amount of damaged metal of red color in the rim of the sample.

The frequency of a Raman (or IR) band is determined by the masses of the atoms in a molecule or crystal, their equilibrium spatial arrangement, their relative displacements during a vibration, and the bond force constants. The intensity depends on either the change in polarizability (Raman) or dipole moment (IR) during the vibration. Different parts of the same molecule tend to be strongly coupled, so changing a single atom in the molecule can perturb many of its vibrations. This means that a subtle structural change can have a large impact, with the advantage that Raman and IR spectra provide a unique fingerprint for a given molecule in a given conformation; the determination of the vibrational spectrum requires sophisticated computer software, such as that employed in the methodology of this work.

The Raman spectroscopy analysis considered a set of points, which corresponded to attacked and nonattacked areas during the anodic experiment, as seen in Figure 3.

Both areas showed the following spectra with small changes in the structural arrangement as a result of the acetic-acetate effect (Fig. 4).

This effect was verified when the spectra 3, 4, 5, and 6 were compared with 2, taken in the rim and apparently not degraded. From these results, we concluded that the attack did not destroy the coating, only deterioration occurred, and no chemical changes affected the rutile (bands 444 and 608 cm^{-1}), corroborating the well known fact of its high stability.

Highly degraded points by iron oxide, such as 7, showed chemical changes and deterioration of the PET coating, when compared with the nonattacked areas of spectrum 2. Spectrum 12 also corresponded to degraded points of earlier acid-steel reaction, and generally appeared as crusts in orange, and other points showed more significant changes (Fig. 5). It is well known that the Raman spectrum is sensitive to the degree of structural organization, and concerning PET, the C=O (1730 cm^{-1}) and the C—C ring coupled with the C—C chain vibration (1096 cm^{-1} and 1117 cm^{-1}) bands are particularly sensitive. We can observe variations in the widths and intensity ratios for the spectra 7 and 12, which are evidence of the significant changes in the protective coating.

Another set of spectra was determined for the perpendicular analysis to the surface of an oxidation area in a sample of the anodic experiment (point 11 in Fig. 3), and showed the performance of the composite (Fig. 6).

In Figure 6, the band 1730 cm^{-1} showed a decrease in the intensities between the spectra, which was confirmed also by the comparative analysis of the peak intensities (I_{886}/I_{795}) indicating a difference in crystallinity (fraction of trans and gauche

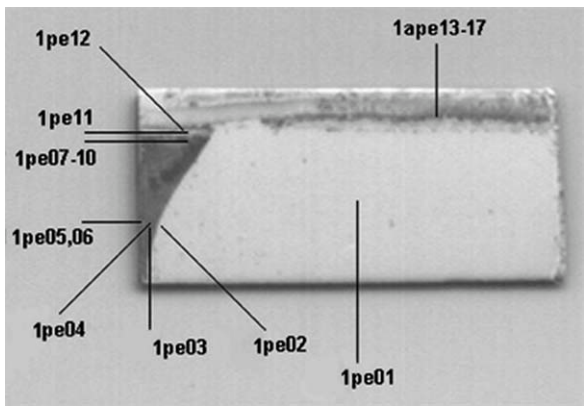

Figure 3 Anodic experiment. General schematic of analysis perpendicular to the surface attacked by the acid medium in sample 1. The titles stand for the spectra nomenclature. Cut 1 – width: 1025 microns; height: 501 microns (1pe01 = Sample 1, perpendicular to point 1). Point 01 is an area showing no evidence of apparent reaction; 02–03 are interfacial damaged/nondamaged areas, 03–10 are areas of reddish color (dark in this figure), 11–17 are areas showing changes in the polymer due to bubbling and color changes by the anodic effect.

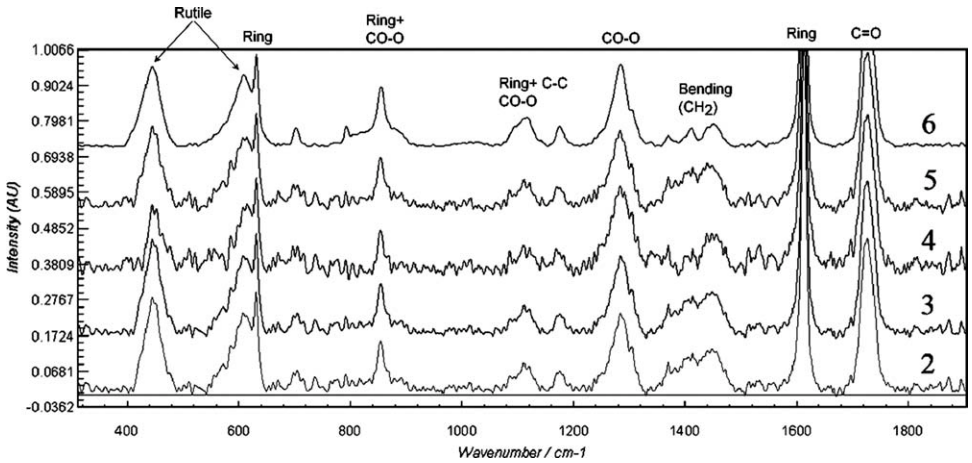

Figure 4 Small changes both in the position and in the profile were observed starting in the interior and extending to the surface. Spectrum 2 is the nonattacked zone; reduced changes can be observed in spectra 3–6, corresponding to areas of the PET damaged by delamination; spectra 7–12 correspond to damaged areas and can be compared with spectrum 2.

conformations of ethylene glycol in the PET structure), considering the variations in the widths of bands and normalization of the spectra.

The cathodic experiments were analyzed by Raman spectroscopy, as described in Figures 7–9. Figure 9 shows that the most significant degradation changes were recorded for the spectrum 5 in bands 1730 cm^{-1}, 1096 cm^{-1}, and 1117 cm^{-1}. The above variations in the intensities and widths of bands are clear indications of changes and structural rearrangements of the PET coating. On the other hand, spectra 4 and 6 did not show significant changes with respect to the reference spectrum of the nondamaged material. In addition, the polymer in the region 1300 to 1500 cm^{-1} also showed structural changes in points 4 and 6 when compared with the nonattacked point 1, where the most altered spectrum was 5; however, these changes were not significant from the point of view of polymer crystallinity referred to the chemical bonds on the PET coating. The most stained and darkest areas resulting from the chemical reaction between the electrolyte (acetic acid) and the steel plate indicated the presence of iron-based compounds in the spectroscopy analyses (Fig. 10).

The Raman spectra showed small variations for the same area of the polymer coating, contaminated by the physicochemical reactions between the electrolyte and the ECCS plate. The spectra obtained confirmed the presence of a mixture of magnetite and goethite, which is the product of the iron oxidation in acidic medium. Magnetite exhibited the characteristic 307 cm^{-1}, 532 cm^{-1}, and 667 cm^{-1} bands, whereas for goethite the characteristic bands detected were 225 cm^{-1}, 297 cm^{-1}, 393 cm^{-1}, 482 cm^{-1}, 565 cm^{-1}, and 676 cm^{-1}.

Also, the spectra were recorded at the contact interface area between the polymer coating and the

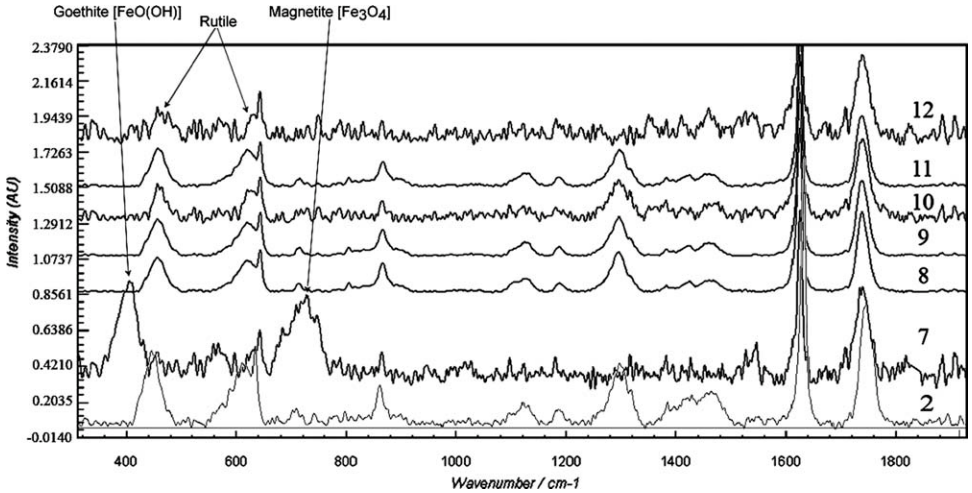

Figure 5 Spectra with evident changes on the PET coating after the anodic experiment.

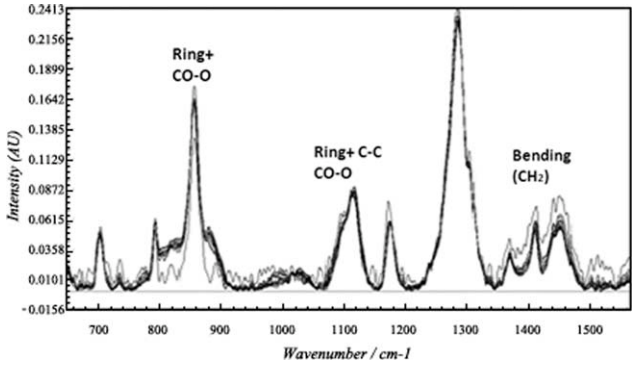

Figure 6 Changes on the PET can also be appreciated in region 700 TO 1500 cm^{-1} and reflect crystallinity alterations of the coating.

metal. In this particular case, they were obtained from an area where no regions of attack to the coating were found. However, some spectral changes starting at the interior and extending to the surface were observed (Fig. 11). Figure 11 recorded the most significant structural changes in the PET coating thickness from the surface to the metal interface. It is well known that in an infrared analysis the peak area in the 1340 cm^{-1} band indicates the presence of the trans conformation in half of the ethylene glycol (CH_2) fragment,[19] and this presence is greater with a volume increase in the crystalline fraction of PET. The two isomers (trans and gauche) in PET can be transformed from one conformation to the other by partial rotation about C—C bonds (1096 cm^{-1} and 1117 cm^{-1} Raman-sensitive bands). It is widely accepted that the conformation in the crystalline phase of PET must be trans, whereas the amorphous phase consists of both trans (extended form) and gauche (relaxed form) isomers. The spectra in Figure 11 evidenced the conformations resulting from the

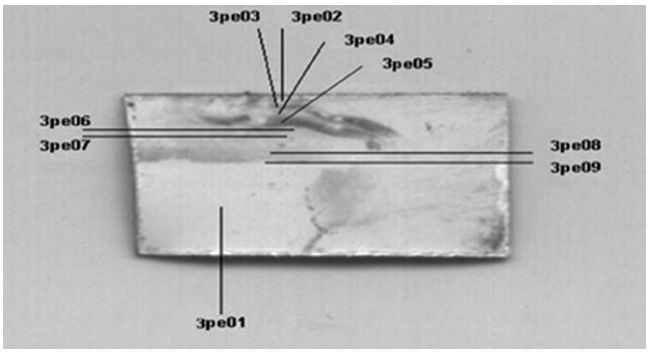

Figure 7 General schematic of analysis perpendicular to the surface attacked by the acid medium in sample (cathodic). The titles stand for the spectra nomenclature. Cut 3 – width: 1237 microns; height: 481 microns. (3pe01 = Sample 3, perpendicular to point 1). Point 01 has not been attacked; points 02–09 correspond to oxidation areas.

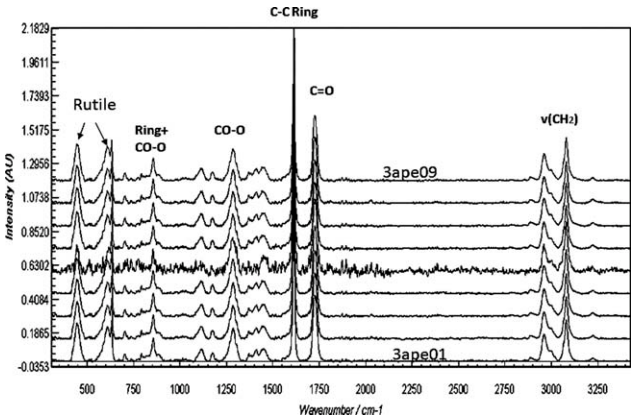

Figure 8 Figure representing the whole spectrum range. The layer observed is the PET coating with TiO_2 (rutile). No important degradations in the coating can be seen, when considering the nonattacked area indicated by spectrum 01 as reference, and compared with the other spectra.

cathodic experiment, and showed changes in the 1267 cm^{-1}, 1456 cm^{-1}, 995 cm^{-1}, 1027 cm^{-1}, and 1096 cm^{-1} bands.

The spectra in Figure 11 were obtained after analyses starting from the PET coating surface until reaching the metal-polymer interface. The cross-section analysis of the PET recorded the following spectra with changes in the region 700 to 1500 cm^{-1}, which reflected in crystallinity variations of the coating, mainly in the band range 1100 cm^{-1}, C—O—CH_2. This last band is also associated with partial rotation changes about C—C bonds making the PET coating more amorphous and affecting the degradation resistance properties to aggressive media.

The changes undergone by the PET coating showed the effect of the induced and accelerated degradation caused by the acetic acetate medium.

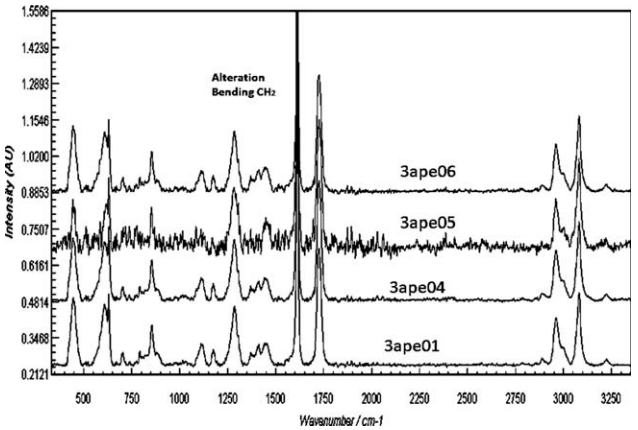

Figure 9 Detail of the points of greater deterioration showing the most altered spectra, mainly in the region 1300 to 1500 cm^{-1}, corresponding to points 01–06 and compared with the nonattacked point 01.

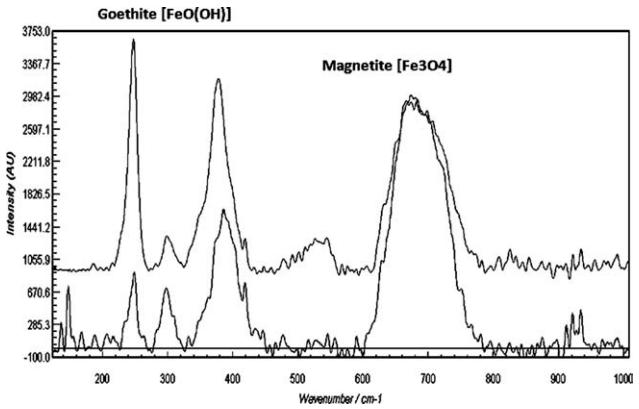

Figure 10 The spectra in points of more intense color on the surface can be interpreted as a mixture of goethite [FeO(OH)] and magnetite [Fe_3O_4]; they correspond to an area perpendicular to the face attacked by the acid and originated in another sample from the cathodic experiment.

The former situation can be minimized under adequate quality control conditions, that is the control of surface defects to favor suitable adhesion, permeability, and layer continuity to prevent the coating from being degraded in a short period of time.

CONCLUSIONS

From the present work, under the experimental and simulated conditions of the study and considering the methodology applied, the following conclusions were drawn:

- The application of an electrochemical cell to generate *in situ* delamination, simulating the formation of pores or artificial defects, provided information on the activity inside the substrates of the PET-coated ECCS composite as a result of the effect of the acetic acid (0.1 g/L acetic acetate buffer solution at pH 3.85).
- The anodic delamination mechanism is based on the diffusion of the electrolyte through the metal-polymer interface and the pre-existence of pores on the polymer layer. In this case, the delamination process is characterized by polymer detachment without separation from the metal substrate, i.e., by metal degradation at the anchorage zone of the polymer layer. The electron microscopy observations of corrosion spots on the metal surface provide empirical evidence of the proposed electrolyte diffusion from the interfacial cross section front toward the interior of the composite.

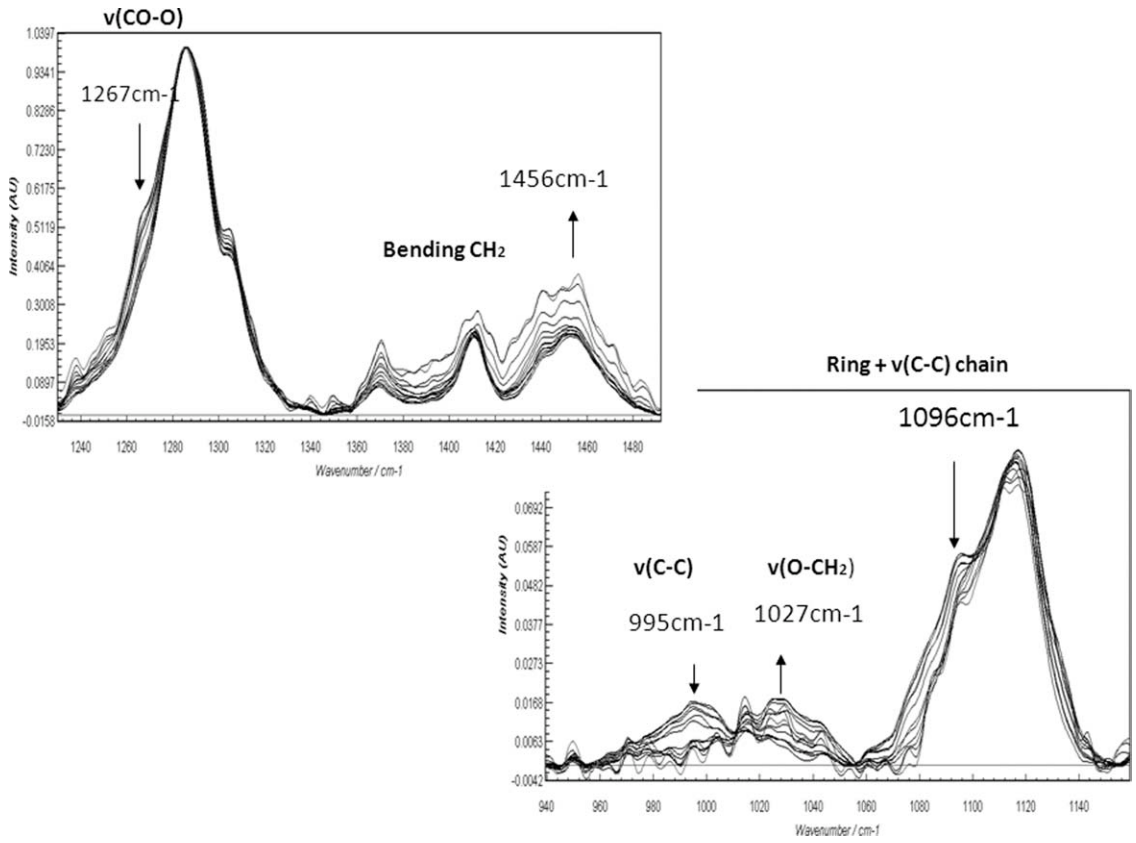

Figure 11 Cathodic experiment. Detail of deformation movements of CH_2 and C—C chains and their evolution in thickness.

- The cathodic delamination mechanism is based on the mechanical action of the gaseous hydrogen as a result of the reduction of H^+. The loss of adherence occurs from the interfacial cross-section to the interior of the coupon, with evidence of polymer separation from the metal substrate of the working sample. The observations indicated no degradation of the metal surface under the polymer coating as a result of the corrosive action of the electrolyte; however, the polymer showed delamination, which did not occur in the anodic experiment.
- The vibrational spectroscopy characterization of the behavior and eventual chemical changes of the ECCS substrates and PET polymer, during the electrochemical experiments performed, allowed to conclude that the anodic delamination mechanism did not destroy the coating from a structural point of view since only partial deterioration or degradation was observed at the points attacked. It is worth mentioning that spectroscopy analyses also detected the presence of rutile (TiO_2), which evidenced no chemical changes in the spectral bands 444 and 608 cm^{-1}.
- The normal surface characterization showed changes in the PET coating crystallinity in the region 700 to 1500 cm^{-1} due to the action of the acetic acid. The profile or thickness analysis of the PET showed no chemical degradation, but localized alterations, from the metal interface toward the surface.
- It is important to emphasize that the intensities of rutile showed a dependency with depth, being its maximum at half of the thickness. The distribution of these pigments in the PET and the coloration of the coating suffered no changes in spite of the acetic acid.
- The spectroscopy analyses of the PET during the cathodic experiment showed no important chemical degradations. The damage was localized as indicated by the normal surface analyses, and a correlation between the most altered areas by the acid and the most altered spectra was observed, corresponding with region 1300 to 1500 cm^{-1}.
- The spectral analysis of the PET coating profile evidenced changes from the steel plate interface area toward the surface; hence, the metal corrosion products were associated with mixtures of goethite and magnetite with variations in color from dark brown to reddish. Whereas the points on the PET most attacked by the acetic acid exhibited changes in crystallinity in the region 700 to 1500 cm^{-1}, which implied changes in the capacity of the protective barrier of the coating.
- The experimental study demonstrated the importance of the control of surface defects and of a good adhesion between the multilayer substrates, since the manufacturing defects favor PET delamination, which can have an early beginning either by cathodic or anodic mechanisms. The latter, implies the possibility of electrolyte diffusion under the polymer, promoting corrosion in pores away from the delamination front.

The authors acknowledged thanks to the special contribution given by Universidad Austral de Chile.

References

1. Baghadachi, J. A. Adhesion Aspects of Polymeric Coatings; Federation of Societies for Coat Technology, Springer, New York, 1996.
2. Corona, E.; Eisenhour, T.; Yin, S.; Mason, J. J. AIP Conf Proc 2004, 712, 964.
3. Szostak, M. Mol Cryst Liq Cryst 2004, 414, 209.
4. Dyer, B. In 7th International Tinplate Conference (ITRI); International Tin Research Institute (ITRI), The Netherlands, 2000; 2–4 October, p 30.
5. Dunnebier, J. C. In ITRI; International Tin Research Institute (ITRI), The Netherlands, Paris, 2004; p 32.
6. Cooper I.; Tice, P. Surf Coat Int 2001, 84, 91.
7. Rastagi, R.; Vellinga, W. P.; Rastogi, S.; Schick, C.; Meijer, H. E. S. J Polym Sci Part B: Polym Phys 2004, 42, 2092.
8. Davidov, A. J Chem Soc Faraday Trans 1991, 87, 913.
9. Mc Gill, W. JOCCA 1977, 60, 121.
10. Chen-his, H.; Schmid, S. R. Wear 2002, 252, 704.
11. Barilli, E.; Fragni, R.; Gelati, S.; Montanari, A. Progress Org Coat 2003, 46, 91.
12. Grundmeyer, G.; Simoes, A. In Encyclopedia of Electrochemistry; Bard, A. J., Stratmann, M., Eds.; Wiley–VCH: Weinheim, 2003; Vol.5, p 500.
13. Rohwerder, M.; Hornung, E.; Sratmann, M. Electrochem Acta 2003, 48, 1235.
14. Vooys, A.; Boelen, B.; Penning, J. P. Prog Org Coat 2009, 65, 30.
15. Zumelzu, E.; Rull, F.; Boettcher, A. J Mater Process Technol 2006, 137, 34.
16. Zumelzu, E.; Cabezas, C.; Alvarado, R. Sci Eng Compos Mater 2006, 13, 1.
17. Zumelzu, E.; Gipoulou, G. T. Surf Coat Int 2002, 85, 1.
18. Zumelzu, E.; Rull, F. Sci Eng Compos Mater 2002, 10, 71.
19. Zumelzu, E.; Rull, F.; Boettcher, A. Surf Eng 2006, 22, 6.
20. Bosch, M. J.; Schreurs, P. J. G.; Geers, M. G. D. J Mater Process Technol 2009, 209, 297.
21. Brewis, D. M.; Critchlow, A. Surf Coat Int 2002, 85, 1.